

# Direct Numerical Simulation of Multiphase Flows with Unstable Interfaces

**Eugenio Schillaci, Oriol Lehmkuhl, Oscar Antepara, Assensi Oliva**

Heat and Mass Transfer Technological Centre (CTTC), Universitat Politècnica de Catalunya (UPC), ESEIAAT, Carrer de Colom 11, 08222, Terrassa (Barcelona), Spain

E-mail: [cttc@cttc.upc.edu](mailto:cttc@cttc.upc.edu)

**Abstract.** This paper presents a numerical model that intends to simulate efficiently the surface instability that arise in multiphase flows, typically liquid-gas, both for laminar or turbulent regimes. The model is developed on the in-house computing platform *TermoFluids*, and operates the finite-volume, direct numerical simulation (DNS) of multiphase flows by means of a conservative level-set method for the interface-capturing. The mesh size is optimized by means of an adaptive mesh refinement (AMR) strategy, that allows the dynamic re-concentration of the mesh in the vicinity of the interfaces between fluids, in order to correctly represent the diverse structures (as ligaments and droplets) that may rise from unstable phenomena. In addition, special attention is given to the discretization of the various terms of the momentum equations, to ensure stability of the flow and correct representation of turbulent vortices. As shown, the method is capable of truthfully simulate the interface phenomena as the Kelvin-Helmholtz instability and the Plateau-Rayleigh instability, both in the case of 2-D and 3-D configurations. Therefore it is suitable for the simulation of complex phenomena such as simulation of air-blast atomization, with several important application in the field of automotive and aerospace engines. A prove is given by our preliminary study of the 3-D coaxial liquid-gas jet.

## 1. Introduction

The study of the liquid atomization process is currently a problem not totally understood in the engineering field, due to the high complexity of the phenomena that lead to the generation and amplification of instabilities at the interface—an introduction to the involved physical processes is available in [1]. A correct numerical representation of such processes would bring great advances in the simulation of important applications, such as automotive engines and propulsion systems. In the last decades, several numerical methods have been proposed, spacing between the three main classes of computational fluid dynamics (CFD) models: in Reynolds-averaged Navier-Stokes equations (RANS) [2], the approach is based on a homogeneous formulation of the two-phase medium, and the transport of mean interface density is modeled by diffusion-like hypothesis, therefore neglecting the effect of the interaction between liquid structures [3]; on the other side, large eddy simulations (LES) approaches [4] still suffer the complexity of coupling turbulence modeling and interface-capturing methods. In particular, many LES models are not able to take into account surface tension forces, that, play a key role in atomization processes [5]. Finally, direct numerical simulation (DNS) approaches involve strict requirements in terms of computational resources, because of the numerous length scales involved in the phenomenon.



That include the correct representation of surface phenomena, such as the growth of waves and filaments, as well as the generation of drops of varying size in primary and secondary atomization processes. Indeed, as demonstrated by [6], the use of huge computational resources is needed to carry out the DNS of complete atomization phenomena. Nevertheless, the quality of the results is excellent, as also demonstrated by other authors, such as [7, 8], that use diverse interface-capturing methods to get accurate representations of turbulent atomization.

In this paper we propose our progress in the DNS of multiphase systems, as well as the introduction of mesh adapting strategies that allow an optimization of computational resources. Recently, other authors have developed similar strategies to reduce the computational requirements for the simulation of multiphase flows [9, 10]. The development of various numerical techniques in our computing platform allowed to study the phenomena responsible for the early surface instabilities, as well as the evolution of secondary structures, as droplets and ligaments, that rise from the destabilized liquids. Our simulations were carried out on both 2-D and 3-D configurations of liquid jets interacting with high speed air fluxes.

## 2. Numerical framework

The numerical model utilized in this work has been developed on the in-house platform *TermoFluids* [11] for CFD simulations, where various improvements have been added to the existing multiphase solver. The scheme adopted includes the finite-volume discretization of the Navier-Stokes equations on 3-D Cartesian or unstructured mesh [12]. In particular, in a domain occupied by two incompressible fluids separated by an interface, the fluids are governed by the following equations

$$\nabla \cdot \mathbf{u} = 0, \quad (1)$$

$$\frac{\partial(\rho\mathbf{u})}{\partial t} + \nabla \cdot (\rho\mathbf{u}\mathbf{u}) = -\nabla p + \nabla \cdot (\mu[\nabla\mathbf{u} + (\nabla\mathbf{u})^T]) + \mathbf{S}, \quad (2)$$

where  $\mathbf{u}$  is the velocity field,  $p$  is the pressure,  $\rho$  is the density,  $\mu$  is the dynamic viscosity and  $\mathbf{S}$  includes the volumetric sources; in this work, only the surface tension is taken into account. The surface tension force,  $\mathbf{S}_\sigma$ , that plays a significant role in the proposed test cases, is discretized by using a continuum surface force (CSF) approach, given in formula by

$$\mathbf{S}_\sigma = \sigma\kappa \left( \frac{\nabla\phi}{\|\nabla\phi\|} \right), \quad (3)$$

where  $\sigma$  is the surface tension coefficient,  $\kappa$  is the curvature and the last term is the normalized gradient of the volume fraction  $\phi$ . The capture of the interface is carried out by means of a conservative level-set method [13]. The interface is advected by means of the following equation

$$\frac{\partial\phi(\mathbf{x},t)}{\partial t} + \nabla \cdot (\phi(\mathbf{x},t)\mathbf{u}) = 0, \quad (4)$$

where  $\phi(\mathbf{x},t)$  is the regularized distance function from the interface —corresponding to the volume fraction used for the evaluation of the surface tension force. Furthermore, at every time step, the level-set function is re-initialized in pseudo-time,  $\tau$ , according to

$$\frac{\partial\phi}{\partial\tau} + \nabla \cdot \phi(1-\phi)\mathbf{n} = \nabla \cdot \varepsilon\nabla\phi, \quad (5)$$

in order to keep the interface sharp and to avoid diffusion. In case of using Cartesian meshes, the adaptive mesh refinement strategy (AMR) is used to dramatically improve the mesh resolution in the vicinity of the interface, thus, allowing an accurate representation of interface phenomena. The algorithm proposed by [14] and extended to multiphase flows in a previous work [15] is here

|        | Re                | We                | $u_g/u_l$ | $M$ |
|--------|-------------------|-------------------|-----------|-----|
| liquid | $1.6 \times 10^4$ | $5 \times 10^3$   |           |     |
| gas    | $2.4 \times 10^6$ | $1.3 \times 10^4$ | 5         | 2.5 |

**Table 1.** Dimensionless numbers of the fluids and inlet velocity ratio in the turbulent 2-D jet.

used. The strategy includes a particular treatment of the mass flows which allows the exact conservation of the mass despite violent changes in the morphology of the mesh. This allows the transport of secondary properties such as momentum and kinetic energy, and consequently, the correct solution of turbulent flows. The refinement process is automatically activated by position sensors, that refine the mesh in the zones in which the interface will move. Moreover, a supplementary sensor can be activated to allow the refinement of the zones with a higher vorticity, in order to improve the solution of the smallest convective scales in turbulent problems.

A hybrid scheme has been used for the discretization of the convective term in the momentum equations. It includes the use of a non-diffusive symmetry preserving operator in the bulk of the phases [16], in order to ensure the proper transport of kinetic energy. On the other hand, a diffusive operator is applied at the interface so as to prevent the growth of spurious currents and preserve the stability of the solution.

### 3. Turbulent Atomization of a 2-D Jet

In this test, the atomization of a 2-D multiphase jet is analyzed, in order to demonstrate the capability of the method to simulate a turbulent physical phenomenon and to show the appearance of Kelvin-Helmholtz instabilities. The test is validated by comparison with the results reported by [9], that performed tests on a correspondent configuration. The set-up, shown in Fig. 1, consists in the injection of two parallel high speed flows (the liquid  $l$ , and the gas,  $g$ ) inside an initially quiet domain. The nature of the resulting jet depends on the dimensionless parameters of the fluids, i.e. the Weber number —fluid inertia over surface tension ratio— and the Reynolds number —fluid inertia over viscous forces ratio— of the  $i$  fluid, defined as

$$\text{We}_i = \frac{\rho_i u_i^2 D}{\sigma}, \quad \text{Re}_i = \frac{\rho_i u_i D}{\mu_i}, \quad (6)$$

where  $D$  is the liquid jet diameter,  $u_i$  is the inlet velocity of the considered fluid, and  $\sigma$  is the surface tension. Another parameter that may influence the physics is the momentum flux ratio,  $M = (\rho_g u_g^2)/(\rho_l u_l^2)$ . The fluids are assigned physical properties so as to obtain the dimensionless numbers reported in Tab. 1; a velocity ratio,  $u_g/u_l$ , equal to 5 is imposed to liquid and gas inlet velocities. The fluids have constant horizontal velocities at the inlet, and, in the case of the liquid, a random component is assigned to the vertical velocity ( $v_l = [-0.1u_l : 0.1u_l]$ ), so as to promote the appearance of instability. At the other boundaries a pressure based condition is applied, in order to mimic an outflow condition. The base mesh counts  $5 \times 10^3$  cells and a second level refinement is used in the simulations—a basic cell can be divided, at most, in 16 sub-cells. The total number of cells rises during the transient jet injection, and, at statistical steady-state, the mesh reaches an average dimension of  $\sim 2.8 \times 10^5$  elements. The mesh is refined in the interface zone, to improve the local definition of surface phenomena. Moreover, the vorticity based criteria is added to refine the mesh in the regions in which a certain vorticity threshold is exceeded, thus, allowing a better solution of the smallest convective scales.

The validation of the case is performed by comparing the results with the ones presented in [9] on a correspondent configuration. For instance, in Fig. 2, a comparison of the time averaged velocity profile,  $u_x$ , is presented for two different distances from the liquid inlet,  $x/D$ . In both cases, good agreement is found with reference data, thus, demonstrating a similar behavior in

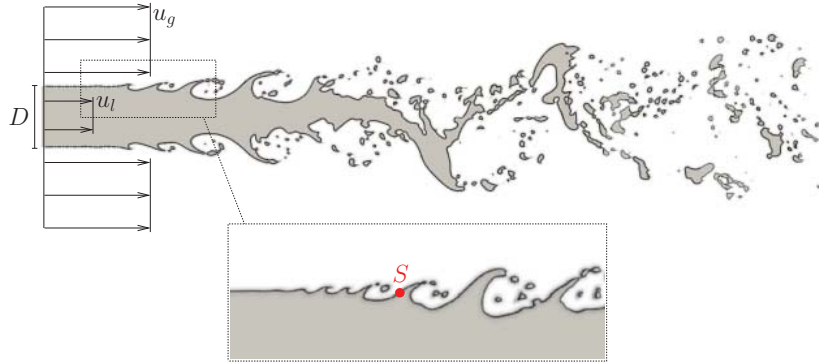


**Figure 1.** Scheme of the 2-D turbulent jet. In the zoom, a particular of the Kelvin-Helmholtz instability mechanism is depicted. The position of the sonde,  $S$ , used to evaluate the energy spectrum is indicated.

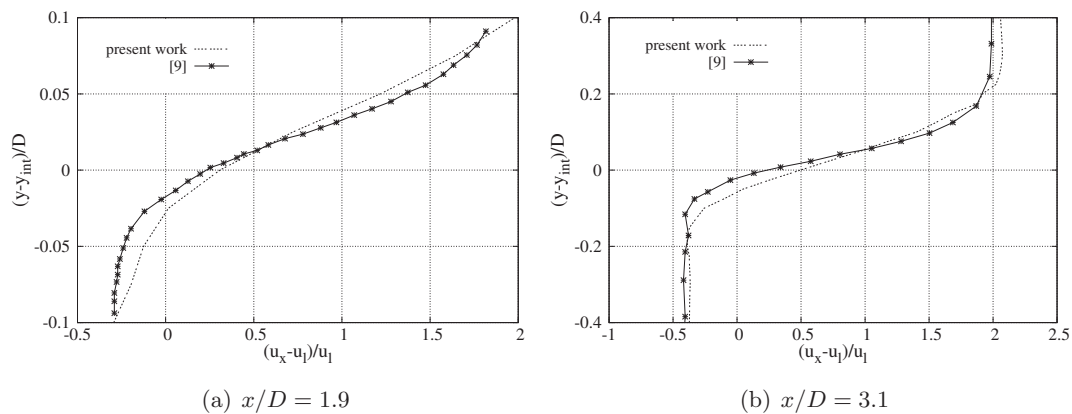


**Figure 2.** Two phase jet: Averaged radial profile of stream-wise velocity,  $u_x$ . Comparison of present data with reference by [9] at two different distances from the inlet,  $x/D$ . Due to the symmetry of the profile, only the top-half part of the profile is represented.  $y_{int}$  indicates the vertical coordinate of the interface position at the inlet.

the zone of early instabilities. The small variance that can be seen in the reported profile is probably due to the different mesh resolution used in the reference work. As can be seen from Fig. 1, the liquid stream is initially disturbed by shear stress due to the difference of speed of the two fluids, corresponding to the Kelvin-Helmholtz instability mechanism. The waves generated on the surface are amplified and quickly generate filaments which break up into small droplets—a detail of this process is depicted in the zoom of Fig. 1. More downstream, instabilities become more violent and lead to the complete rupture of the liquid core, scattering drops of different sizes around the domain.

After a transition phase, the jet reaches a statistical steady-state condition, in which the dispersion of the atomized flow occurs according to a constant frequency of shedding. The energy spectrum of the flow, reported in Fig.3, is obtained by processing the velocity signal—collected at point  $S$  over several shedding cycles—with the Lomb Periodogram technique. The spectrum confirms the existence of a strong vortex shedding frequency, whose peak is situated at  $f_{VS}^* \simeq 0.27$  while several harmonic frequencies can be seen downstream—they are indicated with red circles in Fig.3. Moreover, despite being embedded in the strong fluctuations of the wake,

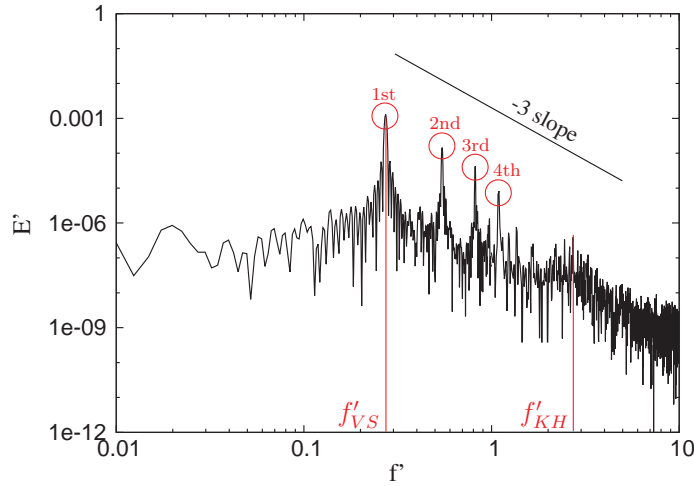


**Figure 3.** Energy spectrum of the 2-D jet evaluated at position  $S$ . The frequencies related to the main oscillation mechanisms,  $f'_{VS}$  and  $f'_{KH}$  are indicated. Red circles indicate harmonic frequencies of  $f'_{VS}$ .

another peak can be isolated in the energy cascade —  $f_{KH}^* \simeq 1.25$  —, indicating the fluctuation mechanism connected to the Kelvin-Helmholtz instability. The overall energy spectrum follows well the -3-slope typical of 2-D turbulent flows [17].

#### 4. Capillary Break-up

The study of the atomization of a three-dimensional complex jet first requires the ability of the numerical method to analyze accurately the processes that occur at the smallest length scales of the problem. In this section we analyzed the instability of a filament, in particular a column of liquid, which, stressed by a surface disturbance, tends to minimize its surface under the action of capillary forces, thus, degenerating into droplets. This phenomenon is commonly called the Plateau-Rayleigh instability. The size of the resulting droplets depend will depend on the component of the sinusoidal perturbation that most quickly grows and causes the break-up of the ligament.

In this test, an unitary liquid column of radius,  $r = 0.1$ , is subjected to a wide cosine wave perturbation, with wavelength,  $\lambda = 1$  and amplitude,  $A = 0.02$  —the initial condition is depicted in Fig. 4 at  $t = 0$ . The simulation is carried out with a second level AMR to reach a local definition at the interface of  $\Delta h = 1/128$ , and the results are compared to the ones proposed by [5] ( $\Delta h = 1/256$  on a static Cartesian mesh). Non-slip boundary conditions are applied to the borders.

The snapshots of Fig. 4 describe the evolution of the flow. In the first stages of the simulation, the filament undergoes a slow deformation, up to approximately  $t = 0.8$ , when it tapers quickly near the edges up to point at which breakage occurs,  $t \simeq 1.0$ . The large central drop, initially deformed, is subjected to a series of oscillations, until it reaches a fully spherical and stable shape, at  $t \simeq 2.0$ . Despite a lower definition of the mesh, our results match very clearly with those of reference.

#### 5. 3-D coaxial Jet at $Re_l = 300$

The configuration of the flux used in the 2-D jet test can be easily extended to the three-dimensional case. In this section, we propose the simulation of an air-liquid coaxial jet

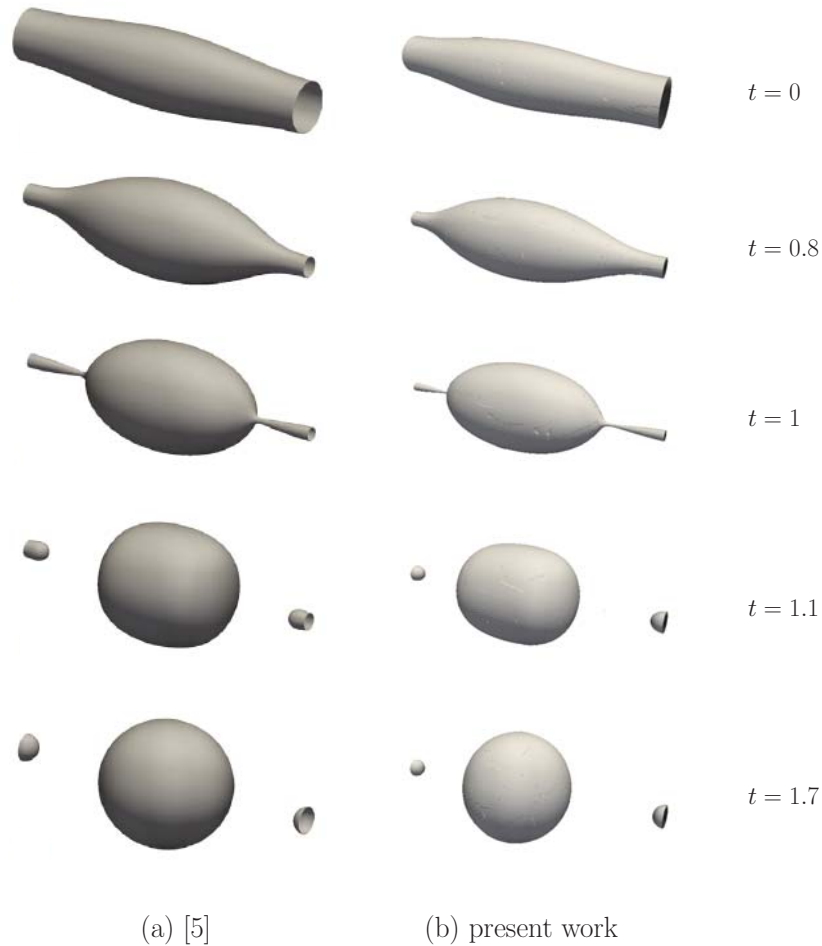


**Figure 4.** Deformation of a liquid column under the effect of the capillary forces. Comparison between our results and reference by [5].

with  $Re_l = 300$ . A circular liquid jet of diameter  $D$  is introduced inside the domain at constant horizontal velocity, surrounded by a coaxial gaseous flow —the physical properties are summarized in dimensionless form in Tab. 2. In this case, no random vertical component were assigned to the inlet fluid. The AMR technique is used to increase the definition of the mesh at the interface up to a second level of refinement. The computational savings in this case are enormous, in fact, starting from a basic mesh of about  $\sim 3.5 \times 10^5$  cells, the size of about  $2.5 \times 10^6$  elements is reached at statistical steady state. Alternatively, the achievement of the same resolution on a static Cartesian mesh would have required the employment of  $\sim 21 \times 10^6$  elements.

|        | Re   | We   | $u_g/u_l$ | $M$ |
|--------|------|------|-----------|-----|
| liquid | 300  | 400  | 5         | 2.5 |
| gas    | 3000 | 1000 |           |     |

**Table 2.** Dimensionless numbers of the fluids and inlet velocity ratio in the 3-D coaxial jet case.

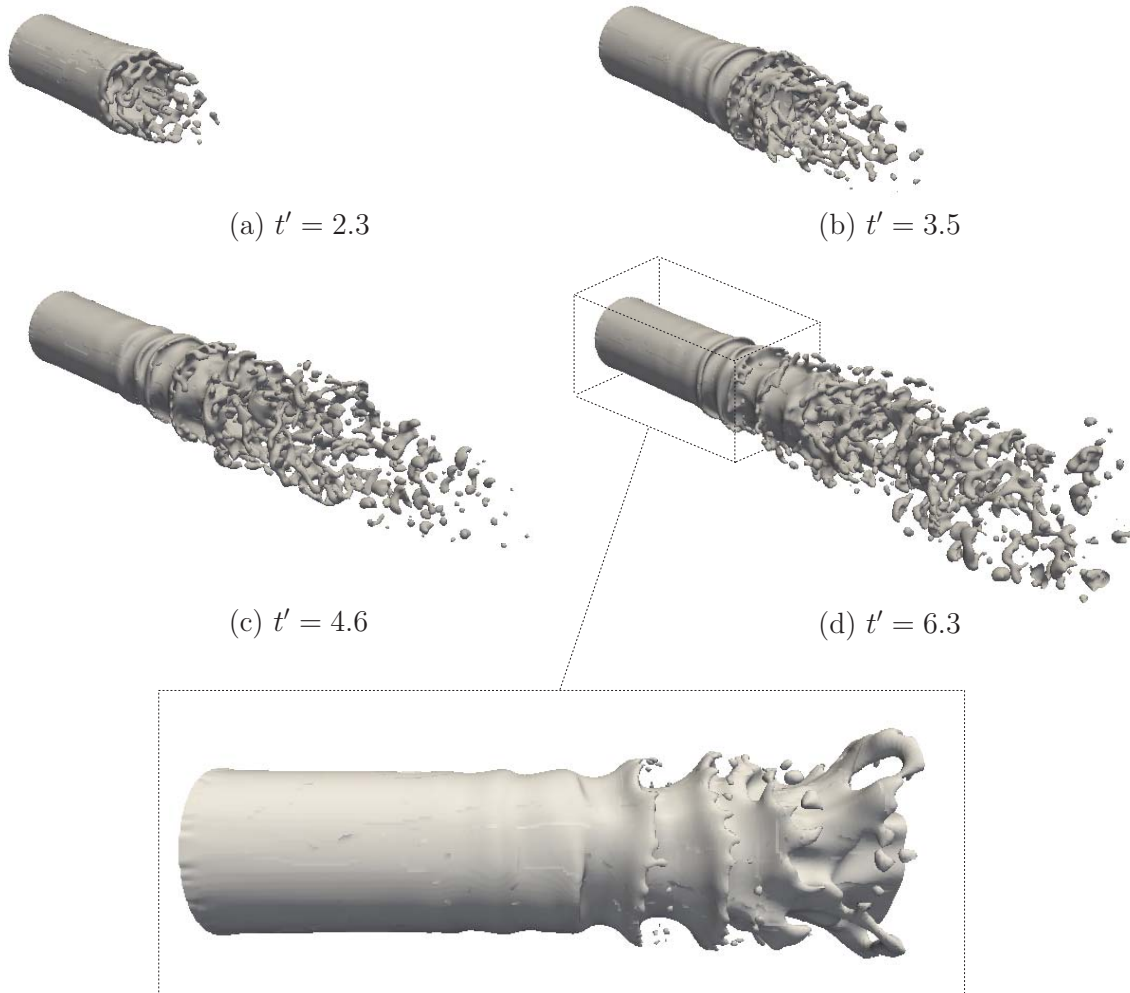


**Figure 5.** Snapshots of the 3-D Jet simulation; the jet surface is first unstabilized by waves, that successively roll-up causing primary atomization. Next, increasingly complex structures rise, including droplets of several different sizes. In the zoom of picture (d), a particular of the Kelvin-Helmholtz instability rise at statistical steady state is shown.

The snapshots of Fig. 5 show the evolution of the jet in the initial stages of the simulation, up to the moment in which the steady state condition is reached. In the zoom of Fig. 5(d), one can observe in detail the Kelvin-Helmholtz mechanism already described in the case of the 2D jet, which leads to destabilization of the surface with the consequent breakage of the liquid core. The liquid then leaves the domain in the form of several different sized particles. Some references to verify the validity of the simulation can be encountered in [18], where several experiments on the coaxial jet set-up are reported. In particular, we can use the following equation to check the length of the intact jet,  $L/D$ ,

$$\frac{L}{D} \simeq \frac{6}{\sqrt{M}} \left(1 - \frac{u_l}{u_g}\right)^{-1}, \quad (7)$$

corresponding to the approximate distance from the inlet where the liquid core totally break-up. The value obtained numerically,  $(L/D = 4.66)_{\text{sim}}$ , coincides well with the empirical one,  $(L/D = 4.75)_{\text{ref}}$ .

## 6. Conclusions and future work

In this paper we have demonstrated the ability of our numerical model to effectively represent some superficial phenomena in multiphase flows. It uses a conservative level set method for the capture of the interface in Cartesian or unstructured meshes. In addition, the model can be coupled with a mesh refinement strategy for the optimization of computational resources. The careful discretization of the Navier-Stokes equations allows the obtainment of a stable method that, by ensuring the conservation of kinetic energy, allows the correct transport of turbulent scales.

In the analyzed cases, we verified the correctness of surface instability that lead to the growth of perturbations and the rise of secondary structures as ligaments and droplets. In future work, we will operate a more detailed study of the 3-D jet —especially in the far field zone where a much finer droplet distribution is present— validating the results with the experimental data provided by [19]. In addition, different jet configurations will be analyzed, such as the liquid injection in still air.

## Aknowledgements

This work has been financially supported by the Ministerio de Economía y Competitividad, Secretaría de Estado de Investigación, Desarrollo e Innovación, Spain (ENE-2014-60577-R), a FI Grant by AGAUR (Generalitat de Catalunya), a PDJ 2014 Grant by AGAUR (Generalitat de Catalunya) and by Termo Fluids S.L.

## References

- [1] Tryggvason G, Scardovelli R and Zaleski S 2011 *Direct numerical simulations of gas-liquid multiphase flows* (Cambridge University Press)
- [2] Vallet A, Burluka A, Borghi R *et al.* 2001 *Atom. Sprays* **11** 619–642
- [3] Gorokhovski M and Herrmann M 2008 *Annu. Rev. Fluid Mech.* **40** 343–366
- [4] Labourasse E, Lacanette D, Toutant A, Lubin P, Vincent S, Lebaigue O, Caltagirone J P and Sagaut P 2007 *Int. J. Multiphas. Flow* **33** 1–39
- [5] Herrmann M 2013 *Comput. Fluids* **87** 92–101
- [6] Shinjo J and Umemura A 2010 *Int. J. Multiphas. Flow* **36** 513–532
- [7] Ménard T, Tanguy S and Berlemont A 2007 *Int. J. Multiphas. Flow* **33** 510–524
- [8] Desjardins O, Moureau V and Pitsch H 2008 *J. Comput. Phys.* **227** 8395–8416
- [9] Fuster D, Bagué A, Boeck T, Le Moyne L, Leboissetier A, Popinet S, Ray P, Scardovelli R and Zaleski S 2009 *Int. J. Multiphas. Flow* **35** 550–565
- [10] Salvador F, Romero J V, Roselló M D and Jaramillo D 2016 *J. of Comput. and Appl. Math.* **291** 94–102
- [11] Lehmkuhl O, Perez-Segarra C, Borrell R, Soria M and Oliva A 2009 TERMOFLUIDS: A new parallel unstructured CFD code for the simulation of turbulent industrial problems on low cost PC cluster *Parallel Computational Fluid Dynamics 2007* (Springer) pp 275–282
- [12] Jofre L, Lehmkuhl O, Ventosa J, Trias F X and Oliva A 2014 *Numer. Heat Tr. B-Fund.* **65** 53–79
- [13] Balcázar N, Jofre L, Lehmkuhl O, Castro J and Rigola J 2014 *Int. J. Multiphas. Flow* **64** 55–72
- [14] Antepara O, Lehmkuhl O, Borrell R, Chiva J and Oliva A 2014 *Comput. Fluids* **110** 48–61
- [15] Schillaci E, Antepara O, Lehmkuhl O, Balcázar N and Oliva A 2015 Effectiveness of adaptive mesh refinement strategies in the dns of multiphase flows *Proceedings of International Symposium: Turbulent Heat and Mass Transfer VIII*
- [16] Verstappen R and Veldman A 2003 *J. Comput. Phys.* **187** 343–368
- [17] Kraichnan R H 1967 *Phys. Fluids* **10** 1417–1423
- [18] Lasheras J and Hopfinger E 2000 *Annu. Rev. Fluid Mech.* **32** 275–308
- [19] Rehab H, Villiermaux E and Hopfinger E 1997 *J. Fluid Mech.* **345** 357–381